2D Closed-Form Solution for the Measurement of the Angle of Attack and Sideslip Angle

Alberto Brandl
Department of Mechanical and Aerospace Engineering
Politecnico di Torino
Torino, Italy
alberto.brandl@polito.it, 0000-0002-6763-4070

Piero Gili
Department of Mechanical and Aerospace Engineering
Politecnico di Torino
Torino, Italy
piero.gili@polito.it, 0000-0002-6868-4547

***Abstract*—At the beginning of 2021, the measurement of the Angle of Attack and of the Angle of Sideslip is still mainly conducted with physical protruding probes. Although several alternative methods have been proposed in literature, the attention is generally focused on data-driven methods and little discussion is conducted on the mathematical problem. If the formulation that allows to associate the aerodynamic angles to other flight parameters has a closed-form solution is still an open question in the field. This paper provides a closed-form solution for a restricted problem where one of the two angle is known. Moreover, a linearized solution is provided. The result section gives evidence of the approach in simulated environment, showing the advantages of the nonlinear solution with respect to the linear one.**

***Index Terms*—angle of attack, estimation, measurement, angle of sideslip, closed form, synthetic sensor**

Glossary

AOA Angle of Attack
AOS Angle of Sideslip
ASSE Angle of Attack and Sideslip Estimator
DOF Degrees of Freedom
MIDAS Modular and Integrated Digital Probe for SAT Aircraft Air Data System
MLP Multilayer Perceptron
SWaP Size, Weight and Power
ULM Ultra Light Machine

I. Introduction

The accurate measurement of Angle of Attack (AOA) and Angle of Sideslip (AOS) is crucial in a lot of flying vehicles. In fact, these two *aerodynamic* angles are tighly coupled with the generation of forces and moments acting on the aircraft. At the time of writing this manuscript, the state of the art of the measurement of the aerodynamic angles consists on the installation of a duplex or a triplex architecture of vanes or multihole probes [1]. A lot of effort has been put into the estimation of these flight parameters without using the protruding probes, in order to monitor the signals measured by the probes, to detect faults or to completely substitute the usage of the mechanical probes with virtual sensors. An example could be the Modular and Integrated Digital Probe for SAT Aircraft Air Data System (MIDAS) project, which is funded by CleanSky 2 with the aim to provide a modular, integrated and digital air data system with the implementation of synthetic sensors for AOA/AOS [2]–[5]. While the MIDAS project is based on Multilayer Perceptron (MLP), Kalman filters have also been extensively applied in this topic [6]–[8]. However, the estimation of AOA/AOS is still an open topic in the aerospace field [9], [10]. In 2020, a mathematical scheme for the estimation of AOA/AOS has been published in [11]. While the scheme is innovative because it actually shows the dependency among the flight parameters, the resulting system of nonlinear equations has been solved numerically. This paper shows a possible closed-form solution of a restriction of the problem. In fact, when one of the two angles is known, a nonlinear equation solvable for the missing angle is obtained. This situation has been identified as bi-dimensional, as it will be described later on. It is interesting to notice that the situation of having only one angle known is not unrealistic. In fact, the sensor architecture might comprise only one traditional probe for reasons related to the Size, Weight and Power (SWaP) requirements or to the accuracy. Another possibility could be a fault on the sensor dedicated to the measurement of one angle, e.g. a failure happens on α and the monitoring system could use the remaining β signal to provide α. The solution proposed in this manuscript, in fact, allows to conduct a cross-check analysis of the aerodynamic angles with a computational inexpensive set of operations. This paper is structured as follows: Sec. II contains a brief introduction to the Angle of Attack and Sideslip Estimator (ASSE) scheme, Sec. III shows the restricted problem and its analytical solution. Some preliminary results are shown in Sec. IV and conclusions are drawn in Sec. V.

II. Background

Similarly to [11], it is possible to express the acceleration of a flying body with respect to an inertial frame I as in (1).

$$\boldsymbol{a}_B = \boldsymbol{C}_{I2B}\boldsymbol{a}_I = \dot{\boldsymbol{v}}_B + \boldsymbol{\Omega}_B\boldsymbol{v}_B + \boldsymbol{C}_{I2B}\dot{\boldsymbol{w}} \tag{1}$$

where $\boldsymbol{a}_i$ stands for the coordinate acceleration of the flying body expressed in the i frame, $\boldsymbol{C}_{I2B}$ is the rotation matrix between the inertial and the Body reference frame, $\boldsymbol{v}_B$ stands for the Body velocity vector with respect to the surrounding air, $\boldsymbol{\Omega}_B$ is the skew-symmetric matrix containing the Body angular rates and $\dot{\boldsymbol{w}}$ is the wind acceleration expressed in the I frame. (1) can be re-arranged to express the time derivative of the Body velocity vector as follows:

$$\dot{\boldsymbol{v}}_B = \boldsymbol{a}_B - \boldsymbol{\Omega}_B \boldsymbol{v}_B - \boldsymbol{C}_{I2B}\dot{\boldsymbol{w}}. \tag{2}$$

Considering the analytical derivation of $\dot{V}_\infty = \frac{\boldsymbol{v}_B^T \dot{\boldsymbol{v}}_B}{V_\infty}$ in (2), the following (3) is obtained.

$$\begin{aligned}\dot{V}_\infty V_\infty = \boldsymbol{v}_B^T \dot{\boldsymbol{v}}_B = \boldsymbol{v}_B^T \left(\boldsymbol{a}_B - \boldsymbol{\Omega}_B \boldsymbol{v}_B - \boldsymbol{C}_{I2B}\dot{\boldsymbol{w}}\right) = \\ = \boldsymbol{v}_B^T \boldsymbol{a}_B - \cancelto{0}{\boldsymbol{v}_B^T \boldsymbol{\Omega}_B \boldsymbol{v}_B} - \boldsymbol{v}_B^T \boldsymbol{C}_{I2B}\dot{\boldsymbol{w}}.\end{aligned} \tag{3}$$

It is now possible to express the relationship between $\boldsymbol{v}_B$ and $\dot{\boldsymbol{v}}_B$ as follows:

$$\boldsymbol{v}_B\left(t\right) = \boldsymbol{v}_B\left(\tau\right) + \int_\tau^t \dot{\boldsymbol{v}}_B\left(\mathcal{T}\right)\, d\mathcal{T} \tag{4}$$

which allows to write (5)

$$\begin{aligned} V_{\infty,\tau}\dot{V}_{\infty,\tau} = \Bigg[\boldsymbol{v}_{B,t} - \int_\tau^t \boldsymbol{a}_B\, d\mathcal{T} + \int_\tau^t \boldsymbol{\Omega}_B \boldsymbol{v}_B\, d\mathcal{T} + \\ + \int_\tau^t \boldsymbol{C}_{I2B}\dot{\boldsymbol{w}}\, d\mathcal{T}\Bigg]^T \left(\boldsymbol{a}_B - \boldsymbol{C}_{I2B}\dot{\boldsymbol{w}}\right)_\tau \Rightarrow V_{\infty,\tau}\dot{V}_{\infty,\tau} + \\ + \left[\int_\tau^t \boldsymbol{a}_B\, d\mathcal{T} - \int_\tau^t \boldsymbol{C}_{I2B}\dot{\boldsymbol{w}}\, d\mathcal{T}\right]^T \left(\boldsymbol{a}_B - \boldsymbol{C}_{I2B}\dot{\boldsymbol{w}}\right)_\tau = \\ = \left[\boldsymbol{v}_{B,t} + \int_\tau^t \boldsymbol{\Omega}_B \boldsymbol{v}_B\, d\mathcal{T}\right]^T \left(\boldsymbol{a}_B - \boldsymbol{C}_{I2B}\dot{\boldsymbol{w}}\right)_\tau . \end{aligned} \tag{5}$$

It is now introduced the assumption that the product $\boldsymbol{\Omega}_B \boldsymbol{v}_B$ varies slowly during a small time interval as follows:

$$\int_\tau^t \boldsymbol{\Omega}_B \boldsymbol{v}_B\, d\mathcal{T} = \left(\boldsymbol{\Omega}_B \boldsymbol{v}_B\right)_t \Delta t, \tag{6}$$

where $\Delta t = t - \tau$. (7) shows the basic expression of the ASSE scheme.

$$\begin{aligned} & V_{\infty,\tau}\dot{V}_{\infty,\tau} + \\ & + \left[\int_\tau^t \boldsymbol{a}_B\, d\mathcal{T} - \int_\tau^t \boldsymbol{C}_{I2B}\dot{\boldsymbol{w}}\, d\mathcal{T}\right]^T \left(\boldsymbol{a}_B - \boldsymbol{C}_{I2B}\dot{\boldsymbol{w}}\right)_\tau = \\ & V_{\infty,t}\hat{\boldsymbol{i}}_{WB,t}^T \left(\boldsymbol{I} - \boldsymbol{\Omega}_{B,t}\Delta t\right)\left(\boldsymbol{a}_B - \boldsymbol{C}_{I2B}\dot{\boldsymbol{w}}\right)_\tau \end{aligned} \tag{7}$$

where

$$\hat{\boldsymbol{i}}_{WB} = \hat{\boldsymbol{i}}_B \cos\beta\cos\alpha + \hat{\boldsymbol{j}}_B \sin\beta + \hat{\boldsymbol{k}}_B \cos\beta\sin\alpha \tag{8}$$

For convenience, it is possible to write (7) in a more compact form (9) as in [11]. The terms h_τ, l_τ, m_τ are detailed in Appendix A.

$$\begin{aligned} n_\tau &= \hat{\boldsymbol{i}}_{WB,t}^T \boldsymbol{m}_\tau = \\ &= h_\tau \cos\beta\cos\alpha + l_\tau \sin\beta + m_\tau \cos\beta\sin\alpha \end{aligned} \tag{9}$$

III. Bi-dimensional Formulation and Closed-Form Solution

From (9) the so-called 2D formulation can be obtained. In fact, suppposing to know α or β, the velocity vector $\boldsymbol{v}_B$ results to be constrained to a plane and it is possible to reduce the problem to a nonlinear equation in the remaining unknown aerodynamic angle. To find a solution, it is possible to take advantage of the parametric formulation for the sine and cosine functions.

A. AOA Solution

Applying the following parametric formulations

$$\sin\alpha = \frac{2s}{1+s^2} \tag{10}$$

$$\cos\alpha = \frac{1-s^2}{1+s^2} \tag{11}$$

where $s = \tan\frac{\alpha}{2}$ with $\alpha \neq \pi + 2k\pi, k \in \mathbb{Z}$, (12) is obtained.

$$\begin{aligned} & \left(h_\tau \cos\beta\right)\frac{1-s^2}{1+s^2} + m_\tau \cos\beta \frac{2s}{1+s^2} = n_\tau - l_\tau \sin\beta \Rightarrow \\ & \Rightarrow \left(n_\tau - l_\tau \sin\beta + h_\tau \cos\beta\right) s^2 - 2 m_\tau s \cos\beta + \\ & \left(n_\tau - l_\tau \sin\beta - h_\tau \cos\beta\right) = 0 \end{aligned} \tag{12}$$

The equation has the following solutions

$$\begin{aligned} s_{1,2} &= \frac{m_\tau \cos\beta \pm \sqrt{\Delta_1}}{n_\tau - l_\tau \sin\beta + h_\tau \cos\beta} \\ \alpha_{1,2} &= 2\tan^{-1}\frac{m_\tau \cos\beta \pm \sqrt{\Delta_1}}{n_\tau - l_\tau \sin\beta + h_\tau \cos\beta} \end{aligned} \tag{13}$$

with $\Delta_1 = \left(m_\tau \cos\beta\right)^2 - \left[\left(n_\tau - l_\tau \sin\beta\right)^2 - \left(h_\tau \cos\beta\right)^2\right]$ and

$$\begin{cases} \left(m_\tau \cos\beta\right)^2 - \left[\left(n_\tau - l_\tau \sin\beta\right)^2 - \left(h_\tau \cos\beta\right)^2\right] \geq 0 \\ n_\tau - l_\tau \sin\beta + h_\tau \cos\beta \neq 0 \end{cases} \tag{14}$$

In the hypothesis of small aerodynamic angles, (9) can be linearised and the solution α' can be found

$$\begin{aligned} & n_\tau - h_\tau \cos\beta - l_\tau \sin\beta = \left(m_\tau \cos\beta\right)\alpha' \Rightarrow \\ & \Rightarrow \alpha' = \frac{n_\tau - h_\tau \cos\beta - l_\tau \sin\beta}{m_\tau \cos\beta} \end{aligned} \tag{15}$$

with $m_t \cos\beta \neq 0$.

The $m_t \cos\beta \neq 0$ condition can be further analysed considering the formulation given in Appendix A. First of all, the linearised solution α' cannot be calculated when $\beta = \frac{\pi}{2} + k\pi, k \in \mathbb{Z}$. Such value for β is actually very rare physically. On the contrary, it is worth noting that with the assumption of steady wind and null angular speed, $m_t \neq 0$ implies $a_Z \neq 0$. This condition has an important impact, preventing the application of the 2D linearised formulation during stationary flight.

B. AOS Solution

The same procedure applied to solve for α can be applied in case β is the unknown variable. Parametric formulations adopted are:

$$\begin{aligned}\sin\beta &= \frac{2s}{1+s^2}\\ \cos\beta &= \frac{1-s^2}{1+s^2},\end{aligned} \tag{16}$$

where $s = \tan\frac{\beta}{2}$ with $\beta \neq \pi \pm 2k\pi$, $k \in \mathbb{Z}$. Therefore, (9) can be factorized and then written as (17).

$$\begin{aligned}&(h_\tau \cos\alpha + m_\tau \sin\alpha)\frac{1-s^2}{1+s^2} + l_\tau \frac{2s}{1+s^2} = n_\tau \Rightarrow\\ &\Rightarrow (n_\tau + h_\tau \cos\alpha + m_\tau \sin\alpha)\, s^2 - 2l_\tau s +\\ &\quad + (n_\tau - h_\tau \cos\alpha - m_\tau \sin\alpha) = 0\end{aligned} \tag{17}$$

The equation has the following solutions

$$\begin{aligned}s_{1,2} &= \frac{l_\tau \pm \sqrt{\Delta_2}}{n_\tau + h_\tau \cos\alpha + m_\tau \sin\alpha}\\ \beta_{1,2} &= 2\tan^{-1}\frac{l_\tau \pm \sqrt{\Delta_2}}{n_\tau + h_\tau \cos\alpha + m_\tau \sin\alpha}\end{aligned} \tag{18}$$

with $\Delta_2 = l_\tau^2 - n_\tau^2 + (h_\tau \cos\alpha + m_\tau \sin\alpha)^2$ and

$$\begin{cases} l_\tau^2 - n_\tau^2 + (h_\tau \cos\alpha + m_\tau \sin\alpha)^2 \geq 0\\ n_\tau + h_\tau \cos\alpha + m_\tau \sin\alpha \neq 0\end{cases} \tag{19}$$

Also in this case, (9) can be linearised according to small aerodynamic angles hypothesis and the linearised solution β' can be found as

$$\begin{aligned}&n_\tau - h_\tau \cos\alpha - m_\tau \sin\alpha = l_\tau \beta' \Rightarrow\\ &\Rightarrow \beta' = \frac{n_\tau - h_\tau \cos\alpha - m_\tau \sin\alpha}{l_\tau}\end{aligned} \tag{20}$$

with $l_t \neq 0$. As done for α', it is possible to analyse the flight conditions corresponding to $l_t \neq 0$. Given the expression of l_t in Appendix A, under the assumption of steady wind and null angular speed, β' cannot be evaluated when $a_Y = 0$, preventing the application of the 2D linearised formulation for stationary flight as for (15).

IV. Numerical Results

Previous sections provide the mathematical background and formulations for the bi-dimensional problem of estimating AOA/AOS. This section shows some results obtained using simulated data. The simulator is a nonlinear coupled 6-Degrees of Freedom (DOF) model with mass, aerodynamic, propulsion and engine characterization based on a Ultra Light Machine (ULM) manufactured in North Italy. The simulation is conducted with numerical integration of the model with explicit Euler scheme, solved at $100\,\mathrm{Hz}$ and the overall simulation covers $75\,\mathrm{s}$ of flight. The aircraft starts from trimmed steady state condition at $800\,\mathrm{m}$ with $V_\infty = 30\,\mathrm{m\,s^{-1}}$, corresponding to $\alpha = 3.98°$, $\beta = -0.09°$ and it is subjected to a doublet on the elevator surface. The entire calculation phase lasted less than $0.1\,\mathrm{s}$ independently from the formulation applied. These numerical results have been obtained with a MATLAB© script on a laptop equipped with i7-7700HQ CPU, 16 GB of RAM. These computational time should be considered very low, compared to the time needed for the 3D nonlinear formulation described in [11]. In fact, in that case, a nonlinear solver has been implemented whereas in this work the formula can be directly computed.

Both nonlinear and linearized formulations proposed in Sec. III have been applied. In case of AOA estimation, the timeseries of the true value and of the estimated values have been superimposed in Fig. 1. As can be seen from Fig. 1, the nonlinear estimation, displayed in red, cannot be distinguished from the true signal, plotted in black. On the contrary, the estimation obtained by linearization of (9) α' loose of accuracy in several cases. Most of them are associated to stationary flight and this provides evidence of the mathematical discussion conducted in Sec. III where it was demonstrated that the 2D linearised formulation cannot be applied during stationary flight when the angular speed is 0. The same comparison has been conducted for the estimation of AOS in Fig. 2. The comparison can be seen from a quantitative point of view in Fig. 3 and 4 which provide more evidence that the nonlinear formulation greatly surpasses in terms of accuracy the estimation obtained using the linearized formulation. The estimation error obtained by (12) is lower than $10^{-3}°$, whereas (17) shows even better results, with an order of magnitude of $10^{-4}°$.

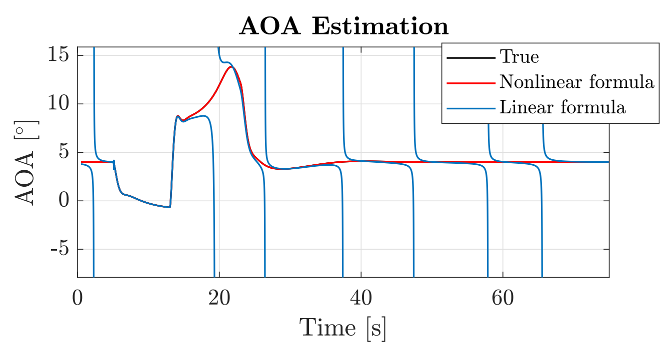

Fig. 1. Timeseries comparison of the proposed estimation methods for AOA, black line is the true value, red line the signal estimated by nonlinear formulation, blue line the signal estimated by linear formulation

To better analyse the estimation error, Fig. 5 shows the distributions of the absolute value of the error in a logarithmic scale. The mean value of the observations is close to $10^{-5}°$ in case of nonlinear formulations, while in case of linear formulation the mean value is affected by the asymptotic trend shown in Fig. 1 and 2.

Although the error of the linearized formulations tends to be higher because of the existence conditions, (15) and (20)

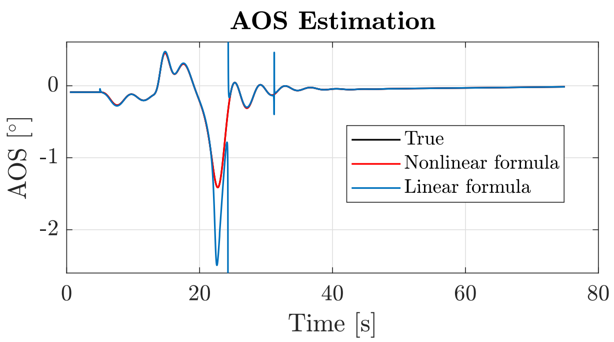

Fig. 2. Timeseries comparison of the proposed estimation methods for AOS, black line is the true value, red line is the signal estimated by nonlinear formulation, blue line is the signal estimated by linear formulation

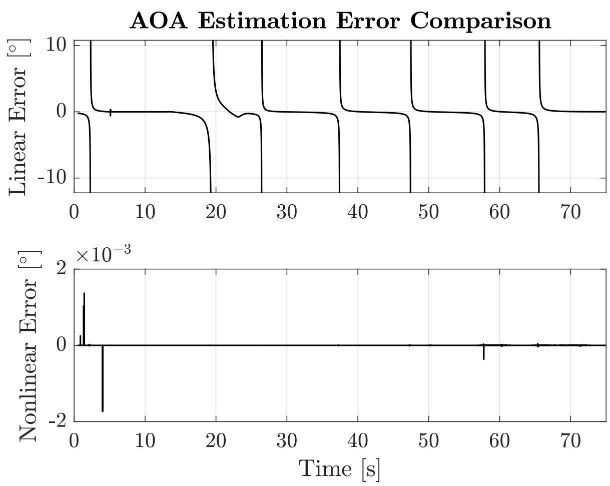

Fig. 3. Estimation error comparison between linear and nonlinear formulation, AOA estimation

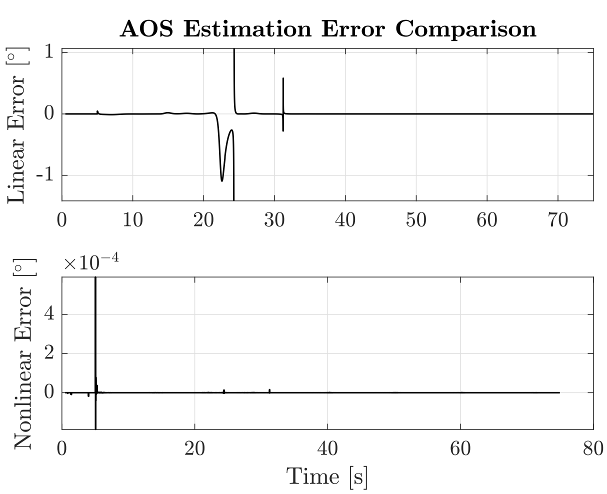

Fig. 4. Estimation error comparison between linear and nonliner formulation, AOS estimation

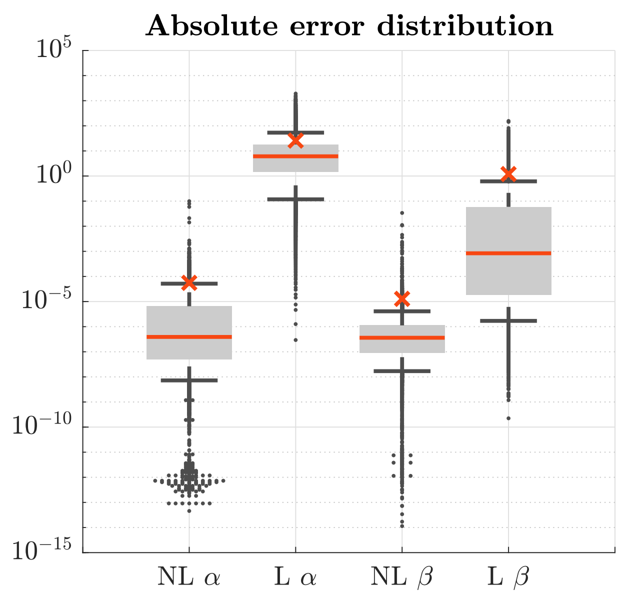

Fig. 5. Comparison of the distributions of the absolute value of the error (crosses stand for the mean value, NL for nonlinear, L for linear)

are still considered valid opportunities when an initial and fast evaluation is needed to drive other estimation algorithms.

V. Conclusion

The accurate measurement of the AOA and AOS is very important for aircraft and other flying bodies. It can lead to improved safety when used in a stall warning device and also it can optimize the control of the aircraft resulting in improved path following capabilities, tracking and fuel consumption. At the time of writing this manuscript, several estimation methods exist but an analytical derivation of the angles is still missing. This paper provides a demonstration that a closed form solution of the estimation of AOA/AOS can be obtained in case of knowledge of one of the two angles. This condition has been referred to as 2D problem, because the velocity vector is contrained to a plane. A numerical demonstration of the method has been given, showing evidence of the approach. The advantage of these formulations is the very low computational time. At the same time, these formulations require the measurement of one of the two angles to be implemented. Moreover, the 2D linearised formulations are limited to unstationary flight. However, the methods shown in this paper can be easily implemented in a more complex architecture, for instance to provide an initial condition to other algorithm, without adding computational burden.

Appendix

The terms h_τ, l_τ, m_τ are introduced in Sec. II to re-write the system of nonlinear equations in a more compact form. This appendix provides the mathematical description of these coefficients, also in case of steady wind field assumption and null aircraft angular speed.

Substituting the definition of $\boldsymbol{\Omega}_{B,t}$, (9) can be expanded as in (21).

$$\begin{aligned}\boldsymbol{m}_\tau = \begin{pmatrix} h_\tau \\ l_\tau \\ m_\tau \end{pmatrix} &= V_{\infty,t} \left(\boldsymbol{I} - \boldsymbol{\Omega}_{B,t}\Delta t\right)\left(\boldsymbol{a}_B - \boldsymbol{C}_{I2B}\dot{\boldsymbol{w}}\right)_\tau = \\ &= V_{\infty,t}\left(\begin{bmatrix} 1 & r\Delta t & -q\Delta t \\ -r\Delta t & 1 & p\Delta t \\ q\Delta t & -p\Delta t & 1 \end{bmatrix}\right) \\ &\left(\begin{pmatrix} a_X \\ a_Y \\ a_Z \end{pmatrix}_B - \boldsymbol{C}_{I2B}\begin{pmatrix} \dot{w}_X \\ \dot{w}_Y \\ \dot{w}_Z \end{pmatrix}\right)_\tau\end{aligned} \tag{21}$$

Assuming a steady wind field, (21) becomes (22).

$$\begin{pmatrix} h_\tau \\ l_\tau \\ m_\tau \end{pmatrix} = V_{\infty,t}\begin{bmatrix} 1 & r\Delta t & -q\Delta t \\ -r\Delta t & 1 & p\Delta t \\ q\Delta t & -p\Delta t & 1 \end{bmatrix}\begin{pmatrix} a_X \\ a_Y \\ a_Z \end{pmatrix}_{B,\tau} \tag{22}$$

Adding the assumption of null angular rates (that is $p = q = r = 0\,\mathrm{s}^{-1}$), (22) eventually reduces to (23).

$$\begin{pmatrix} h_\tau \\ l_\tau \\ m_\tau \end{pmatrix} = V_{\infty,t}\begin{pmatrix} a_X \\ a_Y \\ a_Z \end{pmatrix}_{B,\tau} \tag{23}$$

(21), (22) and (23) can be used to analyse the existence conditions of the solutions of the scheme.

REFERENCES

[1] L. Sankaralingam and C. Ramprasadh, "A comprehensive survey on the methods of angle of attack measurement and estimation in UAVs," *Chinese Journal of Aeronautics*, no. November, nov 2019. [Online]. Available: https://doi.org/10.1016/j.cja.2019.11.003 https://linkinghub.elsevier.com/retrieve/pii/S1000936119304078

[2] A. Lerro, M. Battipede, P. Gili, M. Ferlauto, A. Brandl, A. Merlone, C. Musacchio, G. Sangaletti, and G. Russo, "The clean sky 2 midas project - an innovative modular, digital and integrated air data system for fly-by-wire applications," in *2019 IEEE 5th International Workshop on Metrology for AeroSpace (MetroAeroSpace)*, June 2019, pp. 714–719.

[3] A. Lerro, A. Brandl, M. Battipede, and P. Gili, "Preliminary design of a model-free synthetic sensor for aerodynamic angle estimation for commercial aviation," *Sensors*, vol. 19, no. 23, 2019.

[4] A. Brandl and M. Battipede, "Effects of the wind field on the synthetic measurement of the aerodynamic angles of an aerial vehicle," in *2020 IEEE International Workshop on Metrology for AeroSpace*, 6 2020, pp. 185–190.

[5] A. Lerro and C. Musacchio, "Preliminary definition of metrological guidelines for synthetic sensor verification," in *2020 IEEE International Workshop on Metrology for AeroSpace*, 6 2020, pp. 191–196.

[6] S. Prem, L. Sankaralingam, and C. Ramprasadh, "Pseudomeasurement-aided estimation of angle of attack in mini unmanned aerial vehicle," *Journal of Aerospace Information Systems*, vol. 17, no. 11, pp. 603–614, 2020. [Online]. Available: https://doi.org/10.2514/1.I010783

[7] K. A. Wise, "Computational Air Data System for Angle-Of-Attack and Angle-Of-Sideslip," 2005, uS 6,928,341 B2.

[8] T. J. Rohloff, S. A. Whitmore, and I. Catton, "Air data sensing from surface pressure measurements using a neural network method," *AIAA Journal*, vol. 36, no. 11, pp. 2094–2101, 1998.

[9] W. Youn, H. Lim, H. S. Choi, M. B. Rhudy, H. Ryu, S. Kim, and H. Myung, "State estimation for hale uavs with deep-learning-aided virtual aoa/ssa sensors for analytical redundancy," *IEEE Robotics and Automation Letters*, vol. 6, no. 3, pp. 5276–5283, 2021.

[10] P. Tian, H. Chao, M. Rhudy, J. Gross, and H. Wu, "Wind sensing and estimation using small fixed-wing unmanned aerial vehicles: A survey," *Journal of Aerospace Information Systems*, vol. 18, no. 3, pp. 132–143, 2021. [Online]. Available: https://doi.org/10.2514/1.I010885

[11] A. Lerro, A. Brandl, and P. Gili, "Model-free scheme for angle-of-attack and angle-of-sideslip estimation," *Journal of Guidance, Control, and Dynamics*, vol. 0, no. 0, pp. 1–6, 12 2020. [Online]. Available: https://doi.org/10.2514/1.G005591